Clathrin is required for Scar/Wave-mediated lamellipodium formation

Jérémie J. Gautier[1], Maria E. Lomakina[2], Lamia Bouslama-Oueghlani[3,4], Emmanuel Derivery[1], Helen Beilinson[1], Wolfgang Faigle[3], Damarys Loew[3], Daniel Louvard[3,4], Arnaud Echard[5], Antonina Y. Alexandrova[2], Buzz Baum[6] and Alexis Gautreau[1,3,4,*]

[1]CNRS UPR3082, Laboratoire d'Enzymologie et Biochimie Structurales, Avenue de la Terrasse, 91198 Gif-sur-Yvette Cedex, France
[2]N.N. Blokhin Cancer Research Center of Russian Federation, Kashirskoe shosse, 24, 115478 Moscow, Russia
[3]Institut Curie, Centre de Recherche, 26 rue d'Ulm, 75248 Paris Cedex 05, France
[4]CNRS UMR144, 26 rue d'Ulm, 75248 Paris Cedex 05, France
[5]Institut Pasteur, Membrane traffic and cell division laboratory and CNRS URA 2582, 25-28 rue du Dr Roux, 75724 Paris Cedex 15, France
[6]MRC Laboratory for Molecular Cell Biology and Department of Cell and Developmental Biology, University College London, Gower St, London, WC1E 6BT, UK

*Author for correspondence (alexis.gautreau@lebs.cnrs-gif.fr)

Accepted 20 June 2011
Journal of Cell Science 124, 3414–3427

doi: 10.1242/jcs.081083

Summary

The Scar/Wave complex (SWC) generates lamellipodia through Arp2/3-dependent polymerisation of branched actin networks. In order to identify new SWC regulators, we conducted a screen in *Drosophila* cells combining proteomics with functional genomics. This screen identified Clathrin heavy chain (CHC) as a protein that binds to the SWC and whose depletion affects lamellipodium formation. This role of CHC in lamellipodium formation can be uncoupled from its role in membrane trafficking by several experimental approaches. Furthermore, CHC is detected in lamellipodia in the absence of the adaptor and accessory proteins of endocytosis. We found that CHC overexpression decreased membrane recruitment of the SWC, resulting in reduced velocity of protrusions and reduced cell migration. By contrast, when CHC was targeted to the membrane by fusion to a myristoylation sequence, we observed an increase in membrane recruitment of the SWC, protrusion velocity and cell migration. Together these data suggest that, in addition to its classical role in membrane trafficking, CHC brings the SWC to the plasma membrane, thereby controlling lamellipodium formation.

Key words: Scar/Wave complex, Arp2/3 complex, Actin, Clathrin, Lamellipodium

Introduction

Lamellipodia are protrusions of the plasma membrane that define a leading edge during cell migration (Abercrombie et al., 1970). The membrane is projected through the force provided by actin polymerisation, which can be mainly ascribed to the activity of the Arp2/3 complex that generates branched actin networks (Pollard, 2007). In mammalian cells, the three Wave proteins have emerged as the major activators of the Arp2/3 complex at the leading edge (Insall and Machesky, 2009; Machesky and Insall, 1998; Yamazaki et al., 2003). The small GTPase Rac controls lamellipodium formation through Wave proteins (Miki et al., 1998).

Wave proteins are embedded into multiprotein complexes, the purification of which provided the molecular link between the small GTPase Rac and the Arp2/3 complex (Derivery and Gautreau, 2010; Insall and Machesky, 2009). The canonical Wave complex contains five subunits, namely, Sra, Nap, Abi, Brk1 and Wave (Gautreau et al., 2004; Kobayashi et al., 1998; Machesky et al., 1999). However, like Wave proteins, most subunits of the Wave complex are encoded by paralogous genes, which are variably expressed in different cell types, giving rise to a combinatorial complexity of the Wave complexes that can be assembled (Derivery and Gautreau, 2010). The most ubiquitous Wave complex is composed of Sra1, Nap1, Abi1, Brk1 and Wave2 (Gautreau et al., 2004).

Despite this complexity, a core mechanism regulating Wave complex activity has recently emerged. This mechanism involves Rac and phosphatidylinositol 3,4,5-trisphosphate [PtdIns(3,4,5)P_3]. PtdIns(3,4,5)P_3, the product of phosphoinositide 3-kinase, is produced in response to Rac signalling and further activates Rac in a positive feed-back loop (Weiner et al., 2002; Weiner et al., 2006). PtdIns(3,4,5)P_3 is essential for lamellipodium formation and is involved in recruiting the Wave complex to the plasma membrane through a direct interaction (Oikawa et al., 2004; Sossey-Alaoui et al., 2005). In vitro, the purified Wave complex is inactive (Derivery et al., 2009; Ismail et al., 2009). Addition of GTP-bound Rac at high concentration is sufficient to activate the Wave complex through a conformational exposure of the Arp2/3 activating domain of Wave (Ismail et al., 2009). The membrane, however, plays a crucial role in Wave complex activation, because liposomes containing PtdIns(3,4,5)P_3 and prenylated GTP-bound Rac are much more potent activators than soluble Rac alone (Lebensohn and Kirschner, 2009). In addition to this minimal set of activators, BAR (Bin–amphiphysin–Rvs) domain-containing proteins are involved in Wave complex activation and membrane protrusion (Miki et al., 2000; Suetsugu et al., 2006; Takenawa and Suetsugu, 2007).

In the study reported here we used *Drosophila* cells to identify regulators of the Scar/Wave complex (SWC; Wave is referred to as Scar in this organism). In *Drosophila* cells, a single SWC

exists because each subunit of the SWC is encoded by a single gene, and the SWC controls lamellipodium formation, as in mammalian cells (Ismail et al., 2009; Kunda et al., 2003; Rogers et al., 2003). Using a screen combining proteomics with functional genomics, we found Clathrin heavy chain (CHC) as a protein that binds to the SWC and that regulates lamellipodium formation. These two properties of CHC are conserved from *Drosophila* to mammalian cells. Importantly, we show that the novel function of CHC in lamellipodium formation depends on its ability to promote the recruitment of the SWC to the plasma membrane, but appears independent of its classical role in membrane trafficking.

Results

Identification of CHC as a putative regulator of SWC function in *Drosophila* cells

We reasoned that activators of SWC should both bind to the SWC and produce the characteristic phenotype associated with SWC inactivation. Thus we designed a dual screen in *Drosophila* cells, in which the proteins that bind to the SWC were identified through proteomics and the genes producing the phenotype associated with SWC inactivation were identified upon RNA interference (RNAi)-mediated inactivation. We raised polyclonal peptide antibodies targeting the subunits of the *Drosophila* SWC (supplementary material Table S1). The antibody targeting the Sra1 subunit was very efficient at immunoprecipitating the SWC from *Drosophila* S2 cells (Fig. 1A). A large-scale immunoprecipitation was performed with an excess of lysate so as to saturate the antibody with its specific target and thus to minimise the recovery of cross-reactive proteins. The immunoprecipitate lane was cut in 54 gel slices from top to bottom and each slice was analysed by liquid-chromatography–tandem-mass-spectrometry (LC-MS/MS). This analysis resulted in the identification of 135 *Drosophila* proteins associated with the SWC (supplementary material Table S2). In parallel, we carried out a genome-wide RNAi screen in S2 receptor plus (S2R+) cells for cell shape defects using an established methodology (Kiger et al., 2003). For this purpose, a library of 21,306 distinct double-stranded RNAi (dsRNA) was used. Two immunofluorescences per dsRNA were then individually examined for the morphology of the cell periphery. *Drosophila* cells depleted of the SWC have a characteristic periphery displaying numerous spikes (Kunda et al., 2003; Rogers et al., 2003). Using our genome-wide screen, 35 genes that produced these characteristic spikes upon RNAi-mediated inactivation were identified (Fig. 1B). As expected, genes encoding Arp2/3 complex subunits and the small GTPases, Rac1, Rac2 and Cdc42 were retrieved (Kunda et al., 2003; Rogers et al., 2003). Twenty-eight genes not previously ascribed to this phenotypic class were identified. These genes include those encoding a formin, a SCF ubiquitin ligase complex, proteins previously involved in intracellular traffic, such as clathrin heavy chain (CHC) and dynein light chain, and nuclear factors involved in transcription and RNA metabolism. The other phenotypic classes are reported elsewhere (Rohn et al., 2011). Importantly, the intersection between candidates identified through proteomics and functional genomics contained two gene products, Hrb27C and CHC (Fig. 1C). Hrb27C contains two RRM domains that bind to RNA molecules. Only ambiguous mammalian orthologues, where the homology does not extend beyond the RNA-recognition motif (RRM) domains, were identified. By contrast, CHC is a conserved protein with a well-established function as a vesicular coat component. We thus decided to focus on CHC. Interestingly, the Clathrin light chain was not identified by either screen. We confirmed the phenotype of CHC-depleted cells using S2 cells and an independent non-overlapping dsRNA (Fig. 1D). Indeed, CHC-depleted cells had a spreading defect with the characteristic spikes associated with SWC inactivation. CHC thus fitted the criteria we had defined for a protein potentially regulating SWC function.

CHC depletion, but not several other ways to impair clathrin-mediated trafficking, affects lamellipodium formation

To confirm these results and to identify whether they were repeatable in other organisms, we turned to human HeLa cells, from which the ubiquitous Wave complex has been purified and characterised (Gautreau et al., 2004). Specific co-immunoprecipitation of CHC was detected upon immunoprecipitation of the whole SWC using two independent polyclonal peptide antibodies recognising the Abi1 and Wave2 subunits of the SWC (Fig. 2A). CHC thus co-precipitates with the SWC in both *Drosophila* and human cell lines. HeLa cells normally form a limited number of lamellipodia. To induce them, transient transfection of active Rac, such as the Q61L mutant that is defective in GTPase activity, is often used. However, this procedure gives highly inhomogeneous results because of variable individual levels of expression, precluding accurate quantification. So we turned to the electroporation of the purified Rac1Q61L protein, an experimental system that we previously characterised for the analysis of a precursor in the assembly of the SWC (Derivery et al., 2008). With this method it is possible to introduce a defined dose of protein homogeneously into the cell population. Rac1Q61L was purified and electroporated into HeLa cells in suspension. Cells were then plated in Petri dishes for biochemical analysis or onto coverslips for immunofluorescence analysis. The purified protein indeed entered the cell, as revealed by the increase in total Rac (Fig. 2B). A pulldown experiment using the CRIB domain of PAK indicated that the Rac1Q61L was GTP bound. As expected, this procedure induced a ‘fried egg’ morphology in the vast majority of HeLa cells, with a continuous lamellipodium covering the entire cell periphery (Fig. 2C). This lamellipodium, best revealed by the actin branch marker cortactin (Cai et al., 2008), was associated with the development of radial focal adhesions (supplementary material Fig. S1) and potentiated cell spreading (Fig. 2C).

We then depleted Nap1, a subunit of the SWC, or CHC by transfecting HeLa cells with shRNAs encoding plasmids (Fig. 2D). Nap1 depletion resulted in a destabilisation of the other subunits, Sra1, Wave2, Abi1 and Brk1, as previously described in several organisms and cell types (Derivery and Gautreau, 2010). As expected, CHC depletion impaired transferrin uptake that depends on clathrin-mediated endocytosis (Fig. 2E). We then compared the Rac response of CHC-depleted cells to cells depleted of Nap1. In both CHC- and Nap1-depleted cells, the lamellipodium induced by active Rac was aberrant (Fig. 2C). Instead of being smooth and continuous over the cell periphery, it was frequently interrupted by spikes, which were reminiscent of the spikes observed in *Drosophila* cells, although significantly shorter. Both Nap1- and CHC-depleted cells had a reduced area following Rac electroporation,

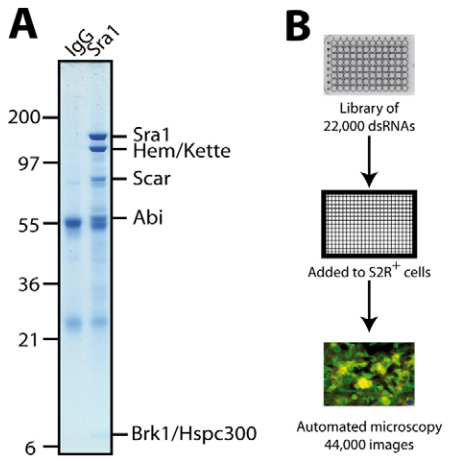

Novel genes producing the Scar phenotype upon RNAi mediated inactivation

FlyBase #	CG #	Acronym	Name	Putative activity or function
FBgn0010333	CG2248	Rac1		Lamellipodium formation
FBgn0014011	CG8556	Rac2		Lamellipodium formation
FBgn0010341	CG12530	Cdc42		Cell polarity
FBgn0031437	CG9881	p16-ARC	Arp2/3 complex subunit 16 kDa	Arp2/3 complex subunit 16 kDa
FBgn0011742	CG9901	Arp14D	Actin related protein 14D	Arp2/3 complex subunit Arp2
FBgn0011744	CG7558	Arp66B	Actin related protein 66B	Arp2/3 complex subunit Arp3
FBgn0001961	CG8978	Sop2	Supressor of profilin 2	Arp2/3 complex subunit 41 kDa
FBgn0052138	CG32138	FMNL2		Formin
FBgn0016984	CG9985	sktl	skittles	Phosphatidylinositol-4-phosphate 5-kinase
FBgn0024196	CG10751	robl	Roadblock	Dynein Light Chain
FBgn0000319	CG9012	Chc	Clathrin Heavy Chain	Vesicular coat component
FBgn0086899	CG34412	tlk	Tousled-like kinase	Serine threonine protein kinase
FBgn0030205	CG17255	nocte	No circadian temperature entrainment	Circadian clock
FBgn0033926	CG12505	Arc1	Activity-regualted cytoskeleton associated protein 1	Response to starvation
FBgn0038350	CG18516			Oxidoreductase
FBgn0039754	CG9747			Fatty acid desaturase
FBgn0031866	CG13772	neuroligin		Neurexin binding
FBgn0023423	CG3412	slmb	Supernumerary limbs	SCF ubiquitin ligase complex
FBgn0015509	CG1877	lin19	lin19 like	SCF ubiquitin ligase complex
FBgn0035136	CG6905	Roc1b		SCF ubiquitin ligase complex
FBgn0002183	CG1828	dre4		Regulation of chromatin assembly
FBgn0000212	CG5942	brm	Brahma	Brahma complex
FBgn0023395	CG9594	Chd3		DNA helicase
FBgn0003345	CG8544	sd	scalloped	Transcription factor
FBgn0028982	CG12225	Spt6		Transcription factor
FBgn0032512	CG9305			Transcritpion factor
FBgn0003415	CG9936	skd	skuld	Transcription mediator complex
FBgn0005411	CG9998	U2af50	U2 small nuclear riboprotein auxiliary factor 50	Nuclear mRNA splicing
FBgn0020497	CG13387	emb	embargoed	Nuclear export
FBgn0004838	CG10377	Hrb27C	Heterogeneous nuclear ribonucleoprotein 27C	Nuclear mRNA splicing/RNA binding
FBgn0036467	CG12310			
FBgn0031249	CG11911			
FBgn0026879	CG13364			
FBgn0039832	CG15563			
FBgn0036454	CG17839			

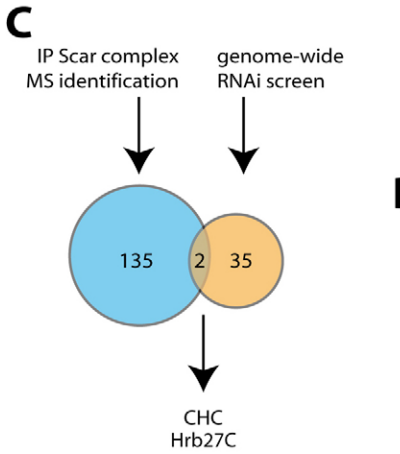

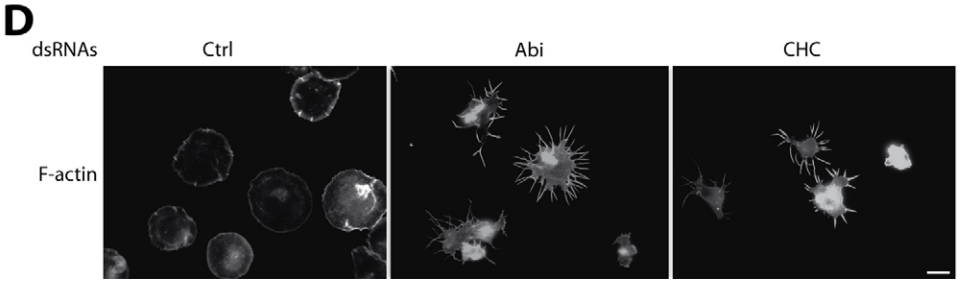

Fig. 1. Identification of CHC as a protein regulating the SWC. (**A**) Lysates from *Drosophila* S2 cells were immunoprecipitated with Sra1 antibody or non-immune IgG. The five subunits of the SWC were detected upon Coomassie Blue staining. Subunits are indicated on the right of the gel and standards, in kDa, on the left. The whole Sra1 lane was analysed by mass spectrometry to identify putative partners of the complex. (**B**) Scheme and results of the RNAi screen. dsRNAs targeting 88% of *Drosophila* genes were used to deplete individual proteins from S2R+ cells. Depleted cells were stained for actin, tubulin and DNA, and pictures automatically taken. Genes found to produce the characteristic phenotype associated with depletion of the SWC, i.e. numerous spikes at the cell periphery, are listed in the table. (**C**) Scheme of the dual screen that identified Clathrin heavy chain (CHC) and Heterogeneous nuclear ribonucleoprotein 27C (Hrb27C) as common candidates of the two approaches. The number of candidates obtained using each approach is indicated. (**D**) Confirmation of the phenotype using an independent dsRNA targeting CHC and a dsRNA targeting the Abi subunit of the SWC as a positive control. Non-adherent S2 cells were spread on concanavalin-A-coated coverslips for 1 hour, and then stained with fluorescent phalloidin. Scale bar: 10 μm.

suggesting that their aberrant lamellipodia are impaired in powering cell spreading (Fig. 2C).

Some cells in the population transfected with shRNA targeting CHC managed to spread efficiently and formed continuous lamellipodia. We observed that these cells with normal lamellipodia were usually the ones less efficiently depleted of CHC (Fig. 3A). We thus decided to quantify the extent of CHC depletion, surface area and spike formation on a cell-by-cell basis. Indeed, the majority of CHC shRNA-transfected cells that exhibited a lower CHC intensity than control cells also had a smaller surface area (Fig. 3B, lower left quadrant). Conversely, the majority of cells transfected with control shRNA showed high CHC intensity and large cell area (upper right quadrant). The phenotype of spike formation was less penetrant than the reduced cell area, because one third of cells efficiently depleted of CHC formed no spikes. However, the remaining two thirds of CHC-depleted cells had five or more spikes, a number that is very rarely reached by control cells (upper left quadrant, Fig. 3B). These observations indicate an agreement between the level of depletion of CHC and the occurrence of these two phenotypes. Similar results were observed with two unrelated shRNA constructs that efficiently targeted CHC (Fig. 3C). Together these results indicate that CHC, like the SWC, is required for lamellipodium formation in human cells, as well as in *Drosophila* cells.

The defect in lamellipodium formation observed upon CHC depletion might be an indirect effect of defective membrane trafficking. Indeed, there are numerous ways in which clathrin depletion could affect lamellipodium formation. For example, signalling growth factor receptors, which trigger lamellipodia, are known to be endocytosed in clathrin-coated pits (Scita and Di Fiore, 2010). This was one of the reasons why we used electroporation of active Rac in the experiments described above rather than growth factor stimulation to analyse lamellipodium formation. Even Rac traffics and the intracellular trafficking of Rac was shown to be important in

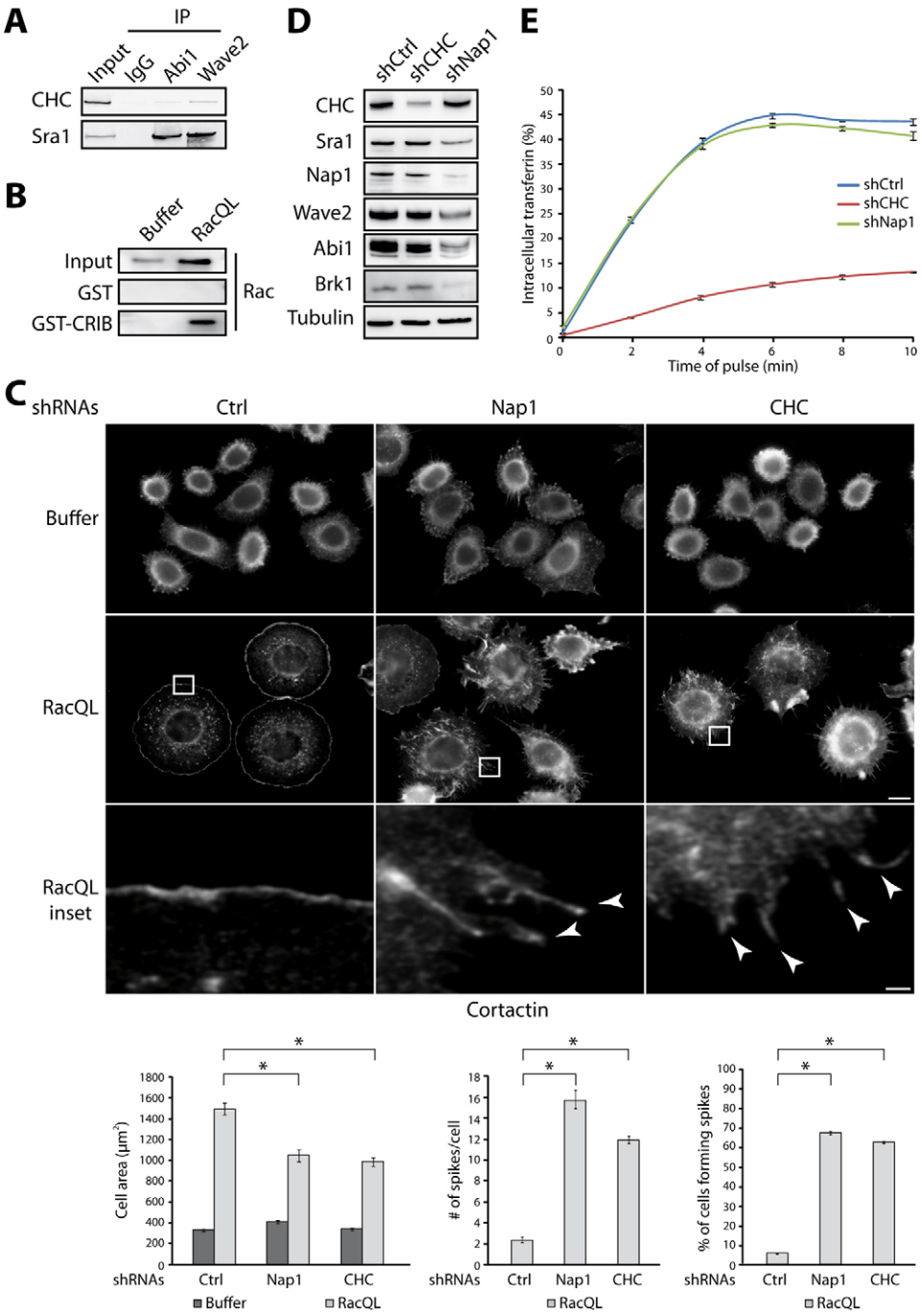

Fig. 2. CHC associates with the SWC and is required for Rac-dependent formation of lamellipodia in HeLa cells. (**A**) Co-immunoprecipitation of endogenous CHC with endogenous Wave complex using either Abi1 or Wave2 antibodies. These two antibodies immunoprecipitate the whole SWC as indicated by the retrieval of a third subunit, Sra1. (**B**) Cells were electroporated with purified Rac1Q61L. The input panel shows the increase of total Rac, and a GST pull-down experiment, using the CRIB domain of PAK, shows that Rac1Q61L is indeed GTP bound. (**C**) Cells were depleted of CHC or Nap1, a subunit of the SWC, by shRNA transfection. Nap1- or CHC-depleted cells were electroporated in suspension with active Rac, replated on collagen-type-I-coated coverslips, allowed to spread for 2 hours and stained with cortactin antibodies. The inset panels are higher magnification images of the boxed regions in the panels above. CHC depletion was associated with defective lamellipodia as indicated by spikes interrupting the circular lamellipodia and the decreased area compared with control cells (values are means ± s.e.m., $n>50$ cells in each condition; $^*P<0.001$). Scale bars: 10 μm; 1 μm inset panels. (**D**) Control of depletion by western blot of whole cell lysates. As expected, Nap1 depletion was associated with a decrease in the levels of all other subunits of the ubiquitous SWC, namely, Abi1, Wave2, Sra1 and Brk1. Tubulin was used as a loading control. (**E**) CHC depletion, but not Nap1 depletion, impairs transferrin endocytosis. Values are means ± s.e.m. of three independent flow cytometry experiments.

order to restrict its signalling to the leading edge of migrating cells (Palamidessi et al., 2008). These findings are likely to explain why the giant lamellipodium induced by exogenous Rac in our assay is isotropic, i.e. not restricted to a leading edge. To examine whether the classical role of clathrin in membrane trafficking has an impact on this new role we describe, lamellipodium formation, we sought to specifically inactivate the role of clathrin in trafficking.

To generate vesicles, clathrin is recruited through different adaptor proteins at various cellular locations (Robinson, 2004). We first used brefeldin A (BFA), which blocks recruitment of coat proteins to membranes, including AP1–clathrin and GGA–clathrin to the trans-Golgi network (TGN) and endosomes, and causes disassembly of the Golgi. Treatment of cells with BFA for 20 minutes resulted in the expected redistribution of the Golgi marker GM130, indicating that the drug treatment was effective (Fig. 4A). This BFA treatment, however, had no effect on lamellipodium formation. We then directly depleted the adaptor complexes AP1 and AP2 using shRNA-encoding plasmids (Fig. 4B). As expected, AP1 depletion impaired steady state distribution of the mannose 6-phosphate receptor, and AP2 depletion strongly impaired transferrin uptake. The depletion of AP1, unlike CHC depletion, did not induce defective lamellipodia, as evidenced by the number of spikes and the Rac-dependent increase in cell area (Fig. 4C). It even had a slightly potentiating effect on the increase of cell area. AP2

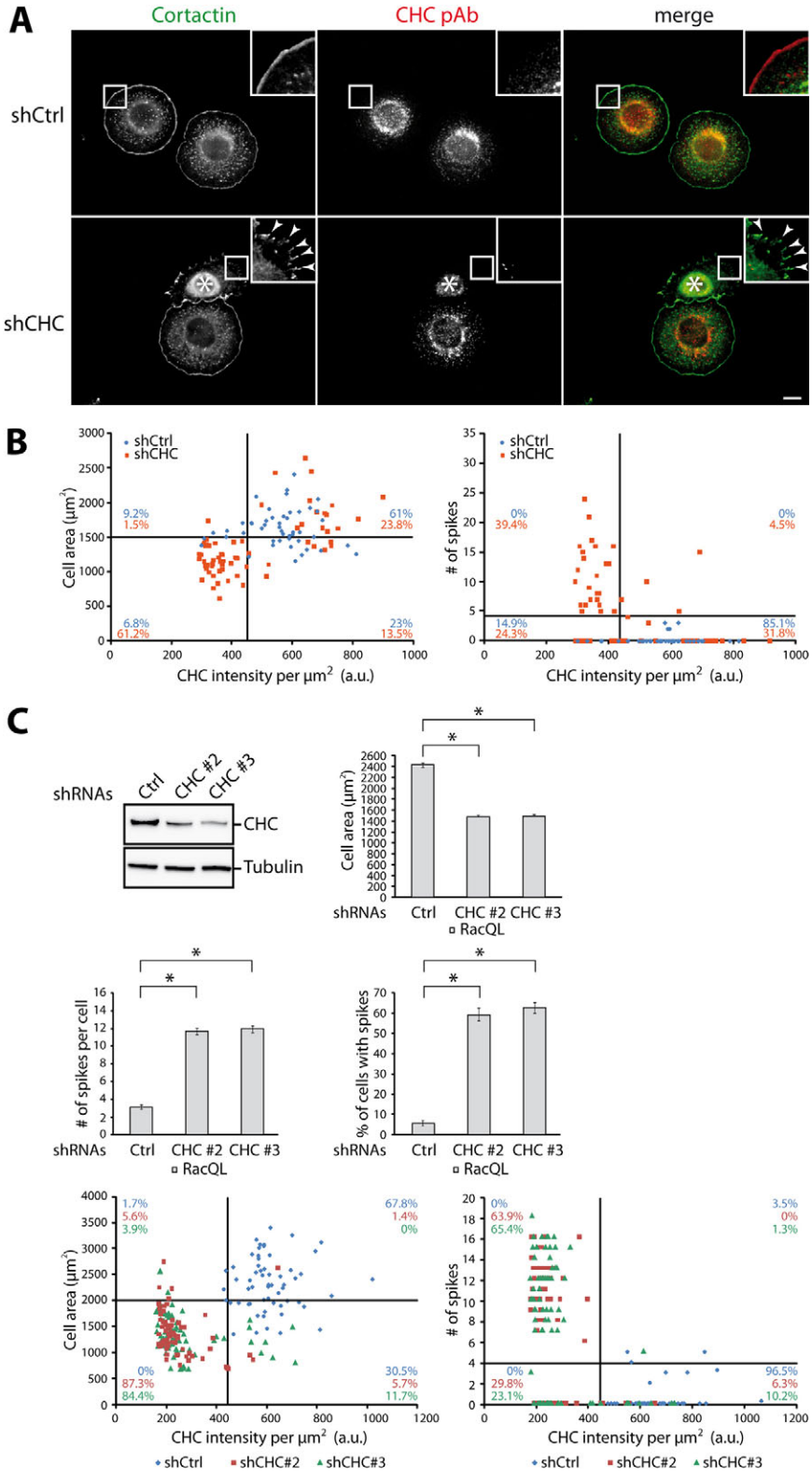

Fig. 3. Defects in lamellipodium formation are associated with the extent of CHC depletion. (**A**) CHC-depleted cells electroporated with Rac1Q61L were analysed by cortactin or CHC immunofluorescence. Only the cell that is efficiently depleted (indicated with a star) has a small surface area and numerous spikes at its periphery. (**B**) Cell-by-cell analysis of cell area, number of spikes and CHC intensity. The coloured numbers indicate the percentage of cells of each category in each quadrant. (**C**) Two additional shRNA constructs targeting CHC have a similar effect on cell area and spike formation; analysed as above (values are means ± s.e.m., $n>50$ cells in each condition; $^*P<0.001$). Scale bars: 10 µm.

depletion had also no detrimental effect on lamellipodium formation, even though the AP2 complex is the adaptor complex that recruits clathrin to the plasma membrane. Altogether these experiments indicate that the effect of clathrin depletion on lamellipodium formation is unlikely to be a secondary consequence of defective trafficking.

CHC localises to the lamellipodium, but is not involved in endocytosis at this location

We sought to colocalise CHC with SWC at the lamellipodium. HeLa cells electroporated with active Rac is not the optimal system for this purpose, because the enrichment of the SWC at lamellipodia is very limited (supplementary material Fig. S1).

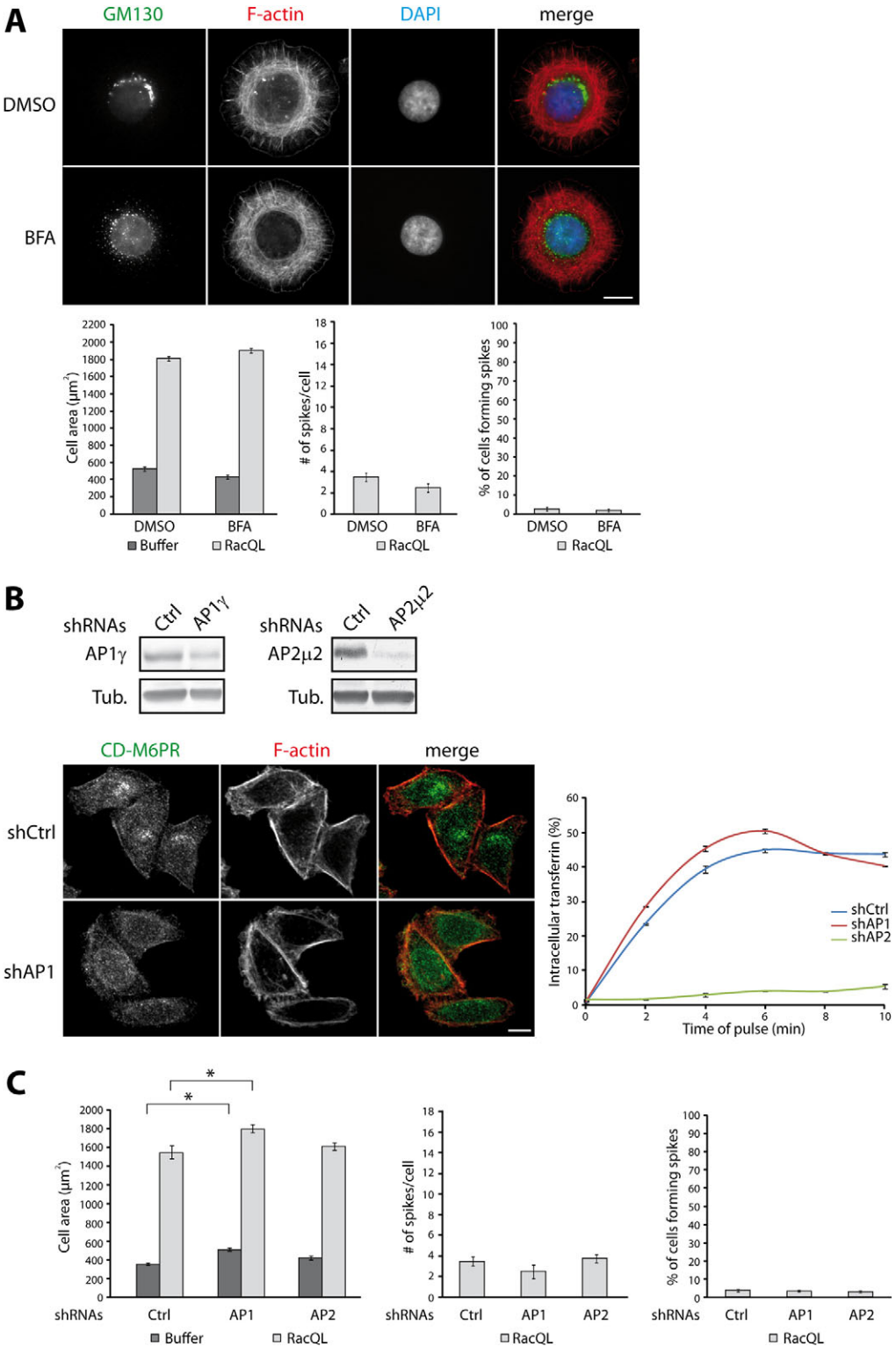

Fig. 4. The role of CHC in lamellipodium formation can be experimentally uncoupled from its role in membrane traffic. (**A**) Treatment of Rac-electroporated HeLa cells with brefeldin A (BFA) for 20 minutes resulted in the expected redistribution of the Golgi marker GM130, but had no effect on lamellipodium formation (values are means ± s.e.m., $n>50$ cells in each condition; $^*P<0.001$). Scale bars: 10 μm. (**B**) Depletion of AP1 and AP2 adaptor proteins from HeLa cells upon shRNA transfection was analysed by western blotting of whole cell lysates. AP1 depletion induced the expected redistribution of cation-dependent mannose 6-phosphate receptor (CD-M6PR). AP2 depletion impaired transferrin endocytosis, as expected (values are means ± s.e.m. of three independent experiments). (**C**) None of these adaptor depletions impaired lamellipodium formation upon Rac electroporation. AP1 depletion even led to an increase in cell area (values are means ± s.e.m., $n>50$ cells in each condition; $^*P<0.001$).

We thus turned to meningioma cells, which spread very efficiently without exogenous Rac. Simple examination of these cells using epifluorescence microscopy reveals an enrichment of cortactin at the periphery (supplementary material Fig. S2A). This enrichment is not observed when a soluble protein, such as RhoGDI, is stained, indicating that enrichment at the periphery is not an artefact due to an increase in membrane thickness in this region. A detectable localisation of the SWC at these lamellipodia was found using Wave2 polyclonal antibody (pAb; Fig. 5) or Brk1 monoclonal antibody (mAb; supplementary material Fig. S2B). Upon depletion of either Wave2 or Brk1, staining of the plasma membrane was lost (supplementary material Fig. S2B,C). X-22 mAb, a well-characterised antibody recognising CHC, also clearly stained

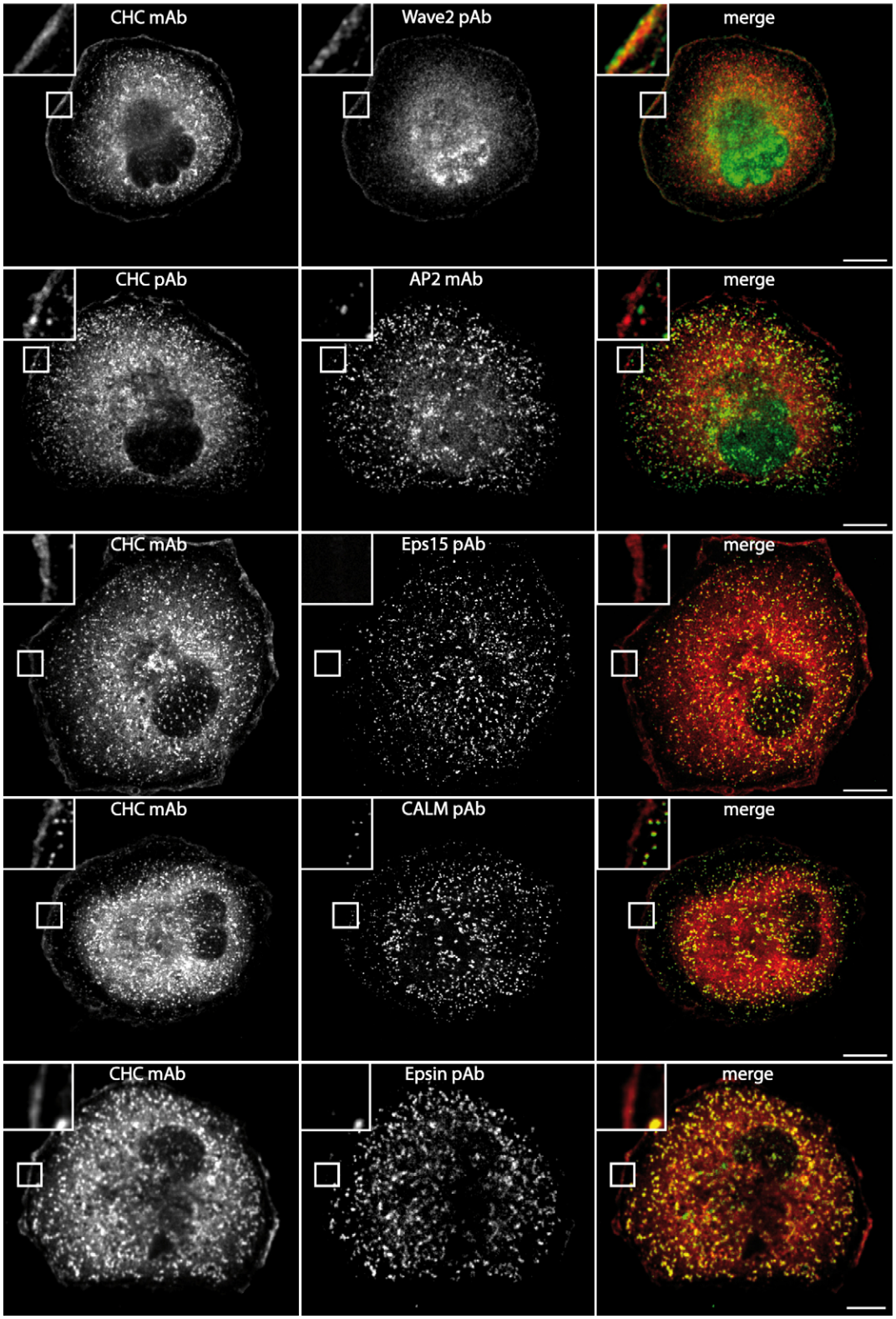

Fig. 5. Clathrin, but not its endocytic adaptor and accessory proteins, colocalises with the SWC in lamellipodia. Meningioma cells were spread on fibronectin-coated coverslips to induce lamellipodia and then stained with the indicated antibodies. A maximum intensity projection of five spinning disk confocal sections is shown. Insets show a magnified view of a peripheral region of a single confocal plane to visualize potential colocalisation. Both pAb and mAb targeting CHC stained lamellipodia. Lamellipodia were stained by Wave2 antibodies, but not by antibodies targeting the endocytic adaptor, AP2, or the endocytic accessory proteins, Eps15, CALM and epsin. With these endocytic markers, colocalisation with CHC was restricted to internal clathrin-coated pits. These results suggest that peripheral CHC is involved in lamellipodium formation, but not in endocytosis. Scale bars: 10 μm.

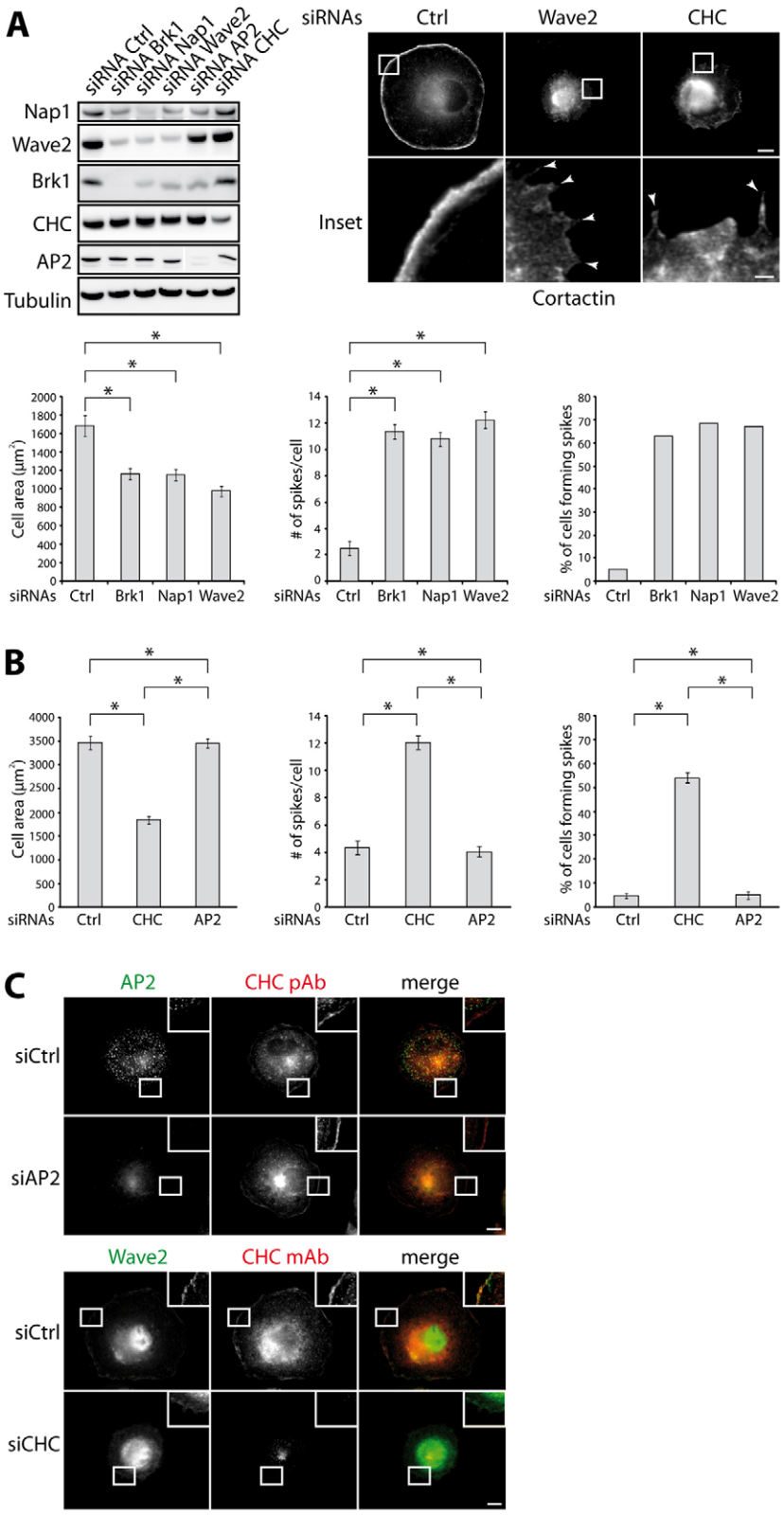

Fig. 6. The peripheral pool of clathrin is required for the formation of SWC-dependent lamellipodia.
(**A**) Meningioma cells were depleted of subunits of the Wave complex (Brk1, Nap1and Wave2), of AP2 or of CHC using transfection of siRNAs. Depleted meningioma cells were spread on fibronectin-coated coverslips to induce lamellipodia, stained with cortactin antibodies and observed by epifluorescence. Depletion of Wave complex subunits resulted in defective lamellipodia as indicated by reduced cell area and spike induction (values are means ± s.e.m., $n>50$ cells in each condition; $^*P<0.001$). (**B**) CHC depletion, but not AP2 depletion, induces defects in lamellipodium formation (values are means ± s.e.m., $n>50$ cells in each condition; $^*P<0.001$). (**C**) Upon AP2 depletion, the peripheral pool of CHC is not affected. Upon CHC depletion, Wave2 is no longer enriched at the plasma membrane. Scale bars: 10 µm or 1 µm in the inset.

lamellipodia. Using confocal sections, we found that CHC colocalises with Wave2. A polyclonal antibody targeting CHC produced similar staining of the lamellipodia. In addition to the lamellipodial staining there was the expected punctuated staining at the ventral membrane using both CHC antibodies (Fig. 5). As expected, both punctate ventral and peripheral stainings obtained with either antibody disappeared upon CHC depletion (supplementary material Fig. S2D). The CHC punctae at the ventral membrane correspond to classical clathrin-coated pits, as indicated by their colocalisation with the adaptor complex AP2

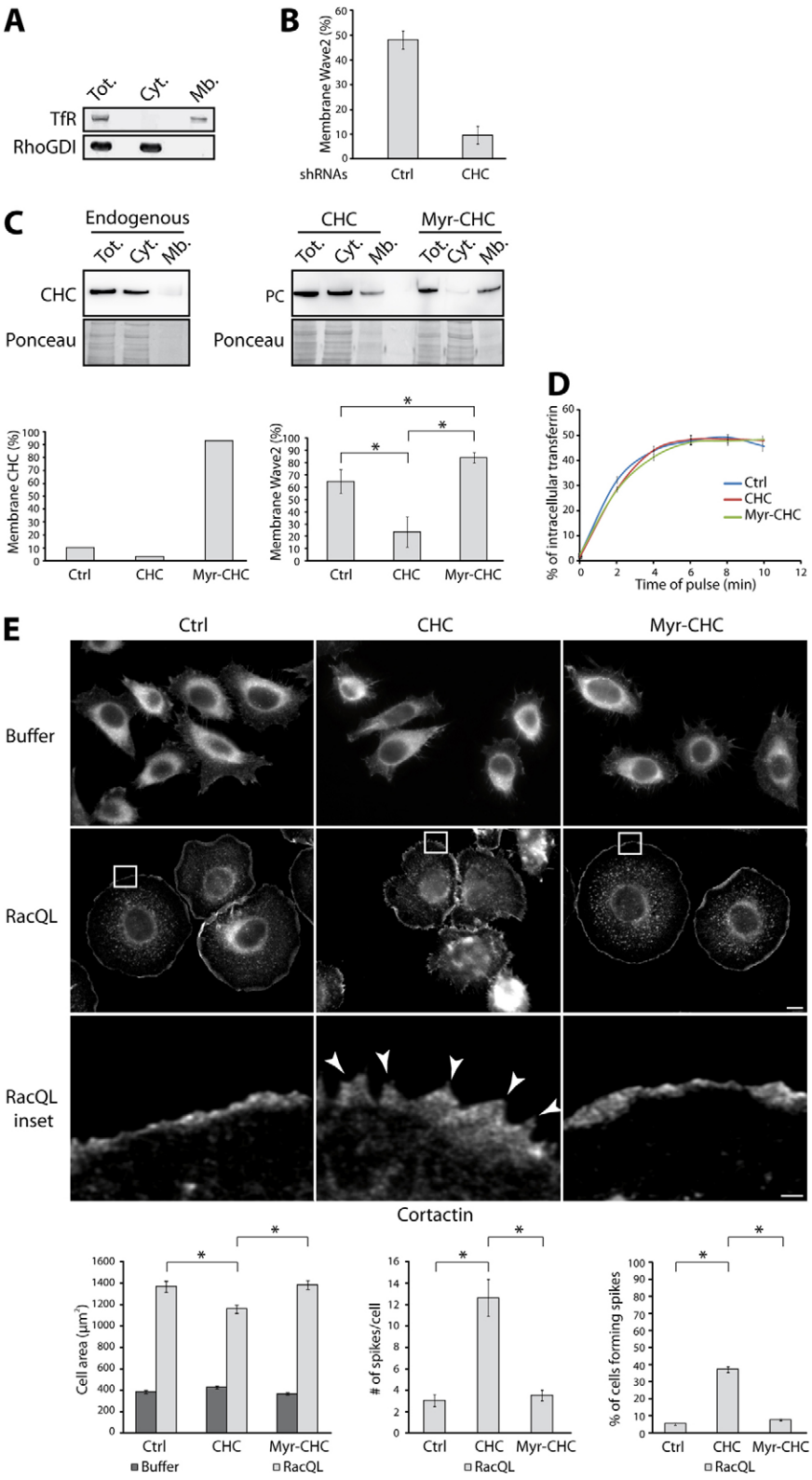

Fig. 7. CHC controls membrane recruitment of SWC. (**A**) HeLa cells were fractionated into cytosol and membrane fractions. Cell fractionation was validated using RhoGDI and transferrin receptor (TfR) as markers of cytosol and membrane fractions, respectively. (**B**) CHC depletion decreased the amount of SWC in the membrane fraction (values are means ± s.e.m. of three independent experiments; *$P<0.001$). (**C**) Expression and membrane distribution of endogenous CHC, PC-tagged CHC and myristoylated PC-tagged CHC. Transfected cells were fractionated. Myr–CHC was mostly bound to membranes, whereas overexpressed CHC was mostly cytosolic. Overexpressed CHC decreased the membrane pool of the SWC, whereas Myr–CHC increased it (values are means ± s.e.m. of three independent experiments; *$P<0.001$). (**D**) Overexpression of CHC or Myr–CHC did not affect clathrin-mediated endocytosis, because transferrin uptake was unaffected. (**E**) CHC overexpression impaired Rac-dependent lamellipodia, as evidenced by the increased number of spikes within lamellipodia and the smaller cell area (values are means ± s.e.m., $n>50$ cells in each condition; *$P<0.001$). The inset panels are higher magnification images of the boxed regions in the panels above. Scale bar: 10 µm or 1 µm in the inset.

and the so-called endocytic accessory proteins, Eps15, CALM and epsin (Fig. 5). The endocytic accessory proteins promote the assembly of the clathrin lattice around endocytic cargoes clustered by AP2. Importantly, none of these endocytic proteins was detected in the lamellipodia with CHC, suggesting that CHC is unlikely to be involved in endocytosis at the lamellipodium.

We depleted meningioma cells of the SWC by transfecting siRNAs targeting either Brk1, Nap1 or Wave2 subunits. Each of

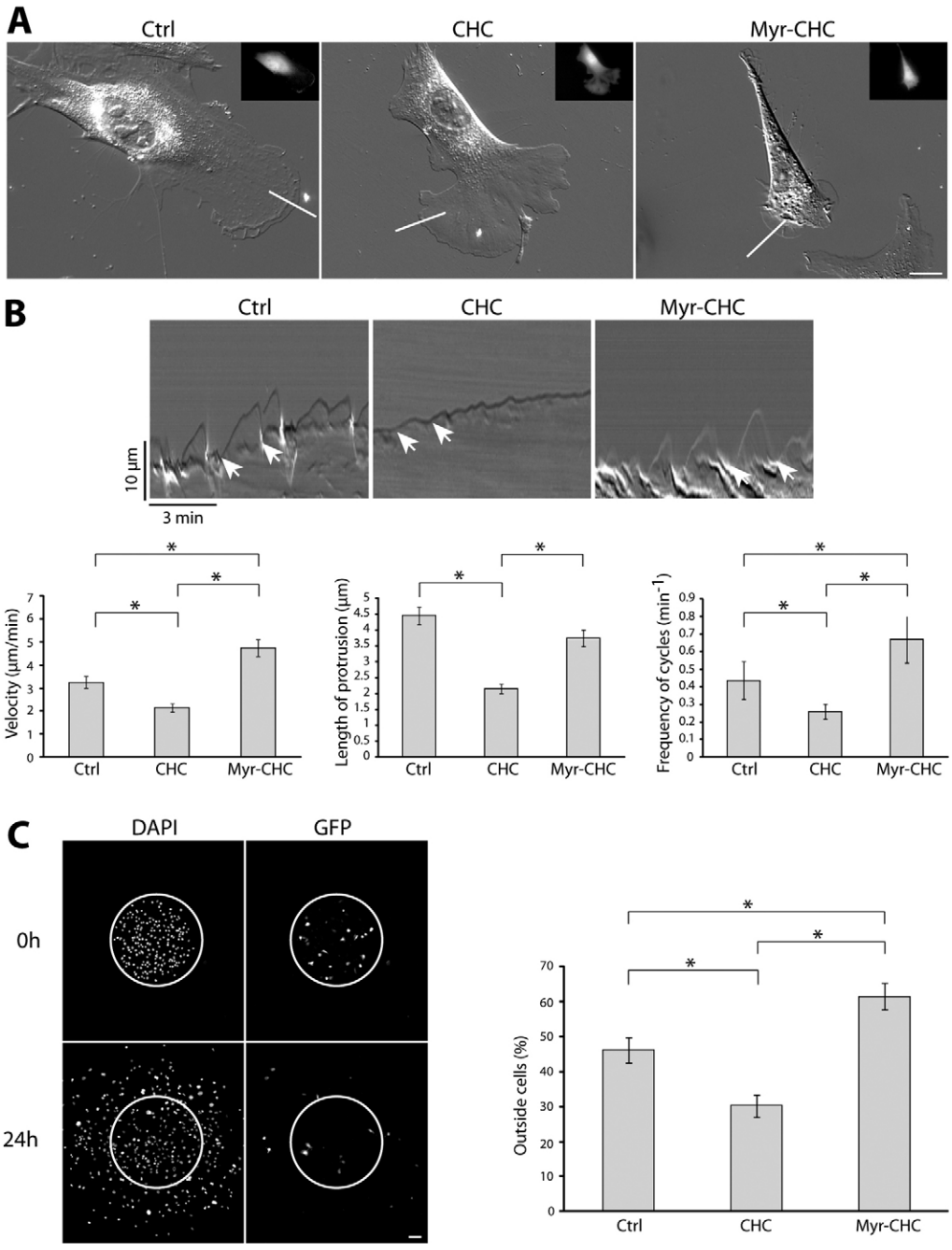

Fig. 8. CHC controls the protrusion rate of leading edges and cell migration. (**A**) Swiss 3T3 cells were transfected with CHC, Myr–CHC or control plasmid together with a GFP-expressing plasmid. Transfected cells, identified by green fluorescence (inset) were observed by DIC microscopy. Scale bar: 10 µm. (**B**) Kymographs show lamellipodial activity along the line orthogonal to the leading edge of the cells shown in A. The beginning and the end of a typical cycle of protrusion and retraction are indicated by white arrows. Velocity was calculated during the protrusion phase of each cycle. In CHC-expressing cells, the length of protrusions decreased and lamellipodia protruded at a lower velocity than in control cells. By contrast, in Myr–CHC-expressing cells, the velocity increased. Furthermore, the frequency of cycles also increased (values are means ± s.e.m., seven cells were analysed per condition, between one and three kymographs per cell, with several protrusive cycles on each kymograph, giving a total of cycles ranging from 38 to 47; *$P<0.001$). (**C**) Swiss 3T3 cells transfected as above were seeded as islands of 700 µm diameter. The number of GFP-positive cells that migrated outside the initial island was counted after 24 hours of incubation. CHC overexpression significantly impaired cell migration, whereas Myr–CHC overexpression potentiated cell migration (values are means ± s.e.m. of six to 19 independent experiments; *$P<0.001$). Scale bar: 100 µm.

these transfections induced defective lamellipodia (Fig. 6A), indicating that lamellipodia depend on SWC in this cellular system as well. We also depleted meningioma cells of CHC or AP2. Similarly to Rac electroporated HeLa cells, CHC depletion, but not AP2 depletion, induced defective lamellipodia (Fig. 6B). This confirmed that the role of CHC in lamellipodium formation does not rely on its function in endocytosis. Accordingly, AP2 depletion did not impair the peripheral staining of CHC (Fig. 6C). This peripheral staining of CHC was also observed by total internal reflection fluorescence (TIRF) microscopy, confirming it was associated with flat lamellipodia (supplementary material Fig. S3). This observation indicates that CHC localisation at lamellipodia is independent from AP2, the most established adaptor complex of endocytosis.

CHC controls membrane recruitment of the SWC, lamellipodium protrusion and cell migration

Wave2 was no longer enriched at the plasma membrane of CHC-depleted meningioma cells, consistent with their defective lamellipodia (Fig. 6C). This observation raised the possibility that CHC controls the distribution of the SWC between the cytosol and the membranes. This was examined using biochemical fractionation of HeLa cells. The procedure we used efficiently separated membranes (both plasma membrane

and endomembranes) from the cytosol, as indicated by the respective markers, transferrin receptor, an integral membrane protein, and soluble RhoGDI (Fig. 7A). Upon CHC depletion, the membrane pool of Wave2 was reduced to approximately a quarter of the level in control cells (Fig. 7B for quantifications; supplementary material Fig. S4A for western blot).

To test whether CHC is able to bring the SWC to the plasma membrane, we fused CHC with an N-terminal myristoylation sequence. Myr–CHC and CHC as a control were tagged with a protein C epitope (PC) to detect their expression. As expected, Myr–CHC was almost completely membrane bound, in contrast to endogenous or exogenous CHC, and indeed, the membrane pool of Wave2 increased upon expression of Myr–CHC (Fig. 7C for quantifications; supplementary material Fig. S4B for western blot). Conversely, the overexpression of wild-type CHC decreased significantly the amount of membrane Wave2. This effect of CHC overexpression was unanticipated, but was even more pronounced than the effect of Myr–CHC. By contrast, the overexpression of CHC or of Myr–CHC had no effect on tranferrin endocytosis (Fig. 7D). Because CHC overexpression decreased the amount of SWC in the membrane fraction, similar to CHC depletion, we expected a defect in lamellipodia formation. Indeed, Rac1Q61L electroporation induced defective lamellipodia in CHC-overexpressing HeLa cells, as evidenced by the increased number of spikes and decreased spreading (Fig. 7E). When overexpressed CHC was targeted to the membrane through myristoylation, these defects were not present. Hence, CHC overexpression uncouples the two functions of CHC. Because CHC overexpression impairs the formation of SWC-dependent lamellipodia without affecting clathrin-mediated endocytosis, we selected this method to assess the role of clathrin in cell migration.

To analyse the role of CHC in migration, we turned to murine fibroblast cells that migrate faster than HeLa cells. Swiss 3T3 cells were transfected with CHC, Myr–CHC or the control plasmid, together with a GFP plasmid to identify transfected cells before time-lapse imaging by DIC microscopy (Fig. 8A). The leading edge activity of these cells was characterised by cycles of protrusion and retraction (supplementary material Movie 1). Retraction occurs when the lamellipodium tip detaches from the substratum and moves backward forming a membrane ruffle. Kymograph analysis of leading edges in transfected cells revealed that CHC overexpression significantly reduced the velocity of lamellipodia, whereas Myr–CHC significantly increased it (Fig. 8B). Myr–CHC expression induced frequent membrane ruffles. By contrast, CHC-overexpressing cells generated significantly shorter protrusions followed by reduced ruffles. The frequency of ruffles in CHC-expressing cells was also half that in Myr–CHC-expressing cells. These observations are, therefore, perfectly in line with the respective effects of these constructs on membrane recruitment of the SWC, which is essential for the generation of a branched actin network that projects the plasma membrane (Derivery and Gautreau, 2010; Suetsugu et al., 2006).

To examine how these defects in lamellipodium protrusion affect cell migration, we used an assay, in which islands of cells were seeded through a microfluidic device perforated with holes of 700 μm in diameter. Swiss 3T3 cells were transfected as above with CHC, Myr–CHC or a control plasmid in combination with a GFP plasmid. The islands were fixed and examined after seeding or after incubation for 24 hours. GFP-expressing cells were then counted. CHC overexpression significantly decreased the number of cells migrating outside the initial island compared with the control, whereas Myr–CHC expression significantly increased the number of migrating cells (Fig. 8C). The ability of these cells to migrate is thus associated with the velocity of protrusions and the amount of SWC at the membrane.

Discussion

The dual screen we conducted using *Drosophila* cells was aimed at identifying novel regulators of the SWC involved in lamellipodium formation. Surprisingly, this screen identified CHC, a major coat protein involved in membrane trafficking. A molecular interaction between the Sra1 subunit of the SWC and CHC was recently reported by Hoflack and colleagues (Anitei et al., 2010). However, they found that this interaction played a role in the generation of tubular carriers derived from the TGN, a classical function for clathrin. By contrast, the atypical function of CHC in lamellipodium formation we report here seems to be independent from its well-established role in membrane trafficking. The evidence against an indirect effect on lamellipodium formation through defective membrane trafficking is threefold. (1) We were able to uncouple the two functions of CHC, using adaptor depletions or BFA. These experiments impaired trafficking, but not lamellipodium formation. (2) Conversely, overexpression of CHC impaired lamellipodium formation, but not trafficking. (3) CHC was detected in lamellipodia without the adaptor and accessory proteins mediating endocytosis. The two functions associated with the complex formed by CHC and SWC, generation of carriers from the TGN and lamellipodium formation, thus appear distinct, even though they share components. These shared components provide a simple explanation of why AP1-depleted cells spread slightly more than control cells in response to Rac (Fig. 4C), because the SWC, which is no longer recruited to the TGN in AP1-depleted cells, can then perform its function at lamellipodia.

The novel function of clathrin in controlling lamellipodia adds to the case for unconventional roles of clathrin. Indeed, clathrin was previously shown to stabilise the mitotic spindle (Royle et al., 2005) and to mediate p53-dependent transcription (Enari et al., 2006). This latter role is also independent of the light chains, as is the role of CHC in lamellipodium formation we describe here. CHC promotes lamellipodium formation through membrane recruitment of SWC. Indeed, our experiments using Myr–CHC suggest that CHC is able to bring the SWC to the membrane. In line with this idea, CHC depletion, or overexpression, greatly decreases the amount of SWC in the membrane pool. This role of clathrin in the recruitment of the SWC to the plasma membrane might explain the recent finding that clathrin is required for actin polymerisation at the immunological synapse (Calabia-Linares et al., 2011), a structure that also depends on SWC activity (Billadeau et al., 2007).

The recent success of reconstituting the activation of purified SWC in vitro using prenylated Rac and liposomes containing PtdIns(3,4,5)P_3 suggest that clathrin is not absolutely required to induce and maintain the active conformation of the SWC (Lebensohn and Kirschner, 2009). The situation is analogous to the one described for BAR-domain-containing molecules of the IRSp53 family, which are crucial in vivo to deform the plasma membrane, to recruit and activate the SWC (Miki et al., 2000;

Suetsugu et al., 2006; Takenawa and Suetsugu, 2007), but which are similarly dispensable in in vitro assays. These results suggest that, even though actin dynamics have been beautifully reconstituted in vitro, the complexity of a lamellipodium, especially its membrane dynamics, has not yet been fully understood and recapitulated in vitro.

It is striking that a major component of the endocytic machinery such as CHC should also be involved in SWC activation and in the formation of lamellipodia. Protrusion of the plasma membrane through actin polymerisation and membrane retrieval through endocytosis are antagonistic. Indeed, biophysical experiments have revealed that either one of these events, but never an unproductive combination of the two, is triggered by the same stimulus, a decrease in membrane tension (Dai et al., 1997; Raucher and Sheetz, 1999; Raucher and Sheetz, 2000). The interaction between CHC and SWC might thus be involved in this coordination by locally shutting down endocytosis in membrane protrusions.

Materials and Methods

Cells and drugs

Drosophila S2 cells were cultured at 26℃ in Schneider's medium containing 10% foetal bovine serum (FBS) and penicillin–streptomycin. When S2 cells were grown in suspension culture using Erlenmeyer's flasks under gentle agitation, the medium was supplemented with 1:100 volume of a 10% Pluronic F-68 solution (Invitrogen). Meningioma, HeLa and 293T cells were cultured in Dulbecco's modified Eagle's medium (DMEM) containing 10% FBS and penicillin–streptomycin. The meningioma cells (#SF1335) used are a surgical isolate from a patient affected by a benign meningioma, a slow-growing tumour arising from arachnoidal cells of the meninges (Rempel et al., 1993). Swiss 3T3 cells were incubated in DMEM supplemented with 5% donor bovine serum. Mammalian cells were incubated at 37℃ in a humidified atmosphere containing 5% CO_2. Brefeldin A (BFA; Sigma) was used at 5 μg/ml for 20 minutes.

RNAi and transfections

Details about the genome-wide screen using S2R+ cells are described elsewhere (Rohn et al., 2011). For RNAi-mediated inactivation, S2 cells were incubated with in vitro produced dsRNAs, as previously described (Bouslama-Oueghlani et al., 2007). dsRNAs were produced from genomic amplified fragments using primers 5′-CTGTACGTGCTCAAGAAAAACG-3′ and 5′-GCATAGGTTCGGGTAGTATTGG-3′ for Abi (CG9749), or 5′-GTGCTTTTCGAGTTTCTGTGC-3′ and 5′-TATCAAAACCGTGGATACTTCG-3′ for CHC (CG9012). These fragments were from an independent library (Echard et al., 2004). S2 cells treated with dsRNA were assayed by spreading on concanavalin-A-coated coverslips as described previously (Rogers et al., 2003). HeLa and 293T cells were transfected with plasmids using electroporation or calcium phosphate precipitation, respectively. Swiss 3T3 fibroblasts were transfected using Lipofectamine LTX and the Plus reagent (Invitrogen). Meningioma cells were transfected with 40 nM On-Target Plus SMART pool (Dharmacon) using lipofectamine RNAi Max (Invitrogen) and analyzed after 4 days. pSuper-Nap1, pSUPER-CHC, pSUPER-AP1γ and pSUPER-AP2μ2 were described previously (Dugast et al., 2005; Saint-Pol et al., 2004; Steffen et al., 2004). For shRNA-mediated RNAi, cells expressed pSUPER plasmids for 3 days. The two additional CHC shRNAs (#2: 5′-TAATCCAATTCGAAGACCAAT-3′; #3: 5′-AATGGATCTCTTTGAATACGG-3′) were cloned into the psiRNA-h7SKblasti G1 plasmid and compared with the so-called scr control plasmid (Invitrogen). For overexpression, cells expressed plasmids for 1 day.

Plasmid constructions

Full-length human clathrin heavy chain (1–1675) was amplified from the IMAGE:6045540 clone and subcloned into custom-made plasmids, pcDNA5 FRT His-PC-TEV or pcDNA5 FRT Myr-PC-TEV between the *Fse*I and *Asc*I sites. This resulted in the fusion of CHC with the N-Terminal peptides, MHHHHHHEDQVDPRLIDGKGGGDYDIPTTENLYFQGAMGRP, or MGSNKSKPKDEDGVDPRLIDGKGGGDYDIPTTENLYFQGAMGRP, respectively. All amplified inserts were verified by sequencing.

Antibodies and immunofluorescence

Anti-human Sra1, Nap1, Wave2 and Abi1 pAbs were described previously (Gautreau et al., 2004). Anti-human Brk1 mAb (clone 231H9) was described previously (Derivery et al., 2008). Anti-tubulin mAb (clone E7) was developed by M. Klymkowsky and obtained from Developmental Studies Hybridoma Bank. Anti-mannose-6-phosphate receptor mAb (22D4) was a kind gift from P. Benaroch (Institut Curie, Paris). The following Abs were from commercial sources: anti-CHC (for western blotting, mAb clone 23, BD Biosciences; for immunofluorescence, mAb X-22 and pAb ab21679, Abcam), anti-AP2μ2 mAb (for western blotting, clone 31/AP50, BD Biosciences), anti-AP2α2 mAb (for immunofluorescence, clone AC1-M11, Abcam), anti-AP1γ (clone 100/3, Sigma), anti-Rac1 mAb (clone 102, Transduction Laboratories), anti-cortactin mAb (clone 4F11, Millipore), anti-transferrin receptor mAb (clone H68.4, Invitrogen), anti-RhoGDI pAb (A-20, sc-360, Santa Cruz), anti-VASP mAb (clone 43, BD Biosciences), anti-paxillin mAb (clone 165, BD Biosciences), anti-CALM pAb (C-18, sc-6433, Santa Cruz), anti-Eps15 pAb (K-15, sc-11716, Santa Cruz), anti-epsin pAb (R-20, sc-8673, Santa Cruz). HRP-conjugated antibodies were from Pierce. Fluorescent phalloidin and Alexa-Fluor-conjugated secondary antibodies were from Molecular Probes. For immunofluorescence, cells were fixed using 3% paraformaldehyde then permeabilised with 0.5% Triton X-100. They were then processed using standard techniques. None of the reported stainings was seen in control experiments, where the primary antibody was omitted.

Cell fractionation

HeLa cells or transfected 293T cells were lysed by nitrogen cavitation (500 psi for 20 minutes; Parr Instruments) in XB buffer (20 mM Hepes, 100 mM KCl, 1 mM $MgCl_2$, pH 7.7) supplemented with protease inhibitor cocktail (Sigma). Debris and nuclei were pelleted by centrifugation at 600 ***g*** for 10 minute at 4℃. The supernatant (total fraction) was then centrifuged for 60 minutes at 150,000 ***g*** using a TLA-100.4 rotor. The supernatant was the cytosolic fraction, and the membrane pellet was solubilised for 60 minutes in radioimmunoprecipitation assay (RIPA) buffer (50 mM Hepes, 150 mM NaCl, 5 mM EDTA, 1% NP-40, 0.5% sodium deoxycholate, 0.1% SDS, pH 7.7) supplemented with protease inhibitor cocktail. The membrane fraction was then centrifuged again for 60 minutes at 150,000 ***g*** to remove insoluble material.

Transferrin uptake

HeLa cells were co-transfected with the plasmid of interest and a GFP-expressing plasmid. Cells were serum starved for 30 minutes in internalisation medium (DMEM, 0.5% BSA, 10 mM Hepes, pH 7.4) at 37℃, washed in PBS and gently detached with trypsin. Cells were then washed with cold internalisation medium. Cells were incubated with Alexa-Fluor-647-conjugated transferrin (5 μg/ml) for 1 hour at 4℃ with gentle agitation. After one wash in cold internalisation medium, cells were resuspended in warm internalisation medium and placed in a 37℃ water bath. An aliquot of cells was taken at each time point and quickly placed on ice in an excess of cold Stop medium (PBS with 0.5% BSA). Cells were then acid washed in 50 mM glycine, 150 mM NaCl, pH 3, on ice for 3 minutes and acidity was neutralised by an excess of Stop medium. After two washes in Stop medium, cells were analyzed by flow cytometry (MoFlo ASTRIOS, Beckman-Coulter). 10^4 GFP-positive cells were analyzed per sample and the geometrical mean fluorescence was determined using Summit software.

Immunoprecipitations

For immunoprecipitations, 10^{10} S2 cells (2.5 l culture, 14 ml cell pellet) were treated for 5 minutes with 1 mM protease inhibitor, di-isopropyl-fluoro-phosphate (Sigma), with appropriate safety procedures. HeLa and S2 cells were lysed in RIPA buffer supplemented with protease inhibitor cocktail (1:1000; Sigma P8340). Extracts were clarified by centrifugation and ultracentrifugation, then incubated with 2 μg non immune rabbit IgG or affinity purified peptide antibodies, together with 10 μl of protein-A-Affiprep beads (Bio-Rad) for 2 hours at 4℃. Beads were then washed four times with RIPA buffer and resuspended in SDS loading buffer. SDS-PAGE was performed with NUPAGE 4–12% Bis–Tris or 3–8% Tris–acetate gels (Invitrogen). Western blots were revealed using HRP-coupled antibodies, Supersignal kit (Pierce) and Fuji LAS-3000 (Fujifilm). Blots were quantified using ImageJ.

Mass spectrometry

Gel slices were reduced, alkylated and subjected to digestion with trypsin (Roche Diagnostics). Extracted peptides were dried and resolubilised in solvent A [95/5 water/acetonitrile in 0.1% (w/v) formic acid]. The total digestion product of a gel slice was used per LC-MS/MS analysis. The extracted peptides were concentrated and separated on a LC-Packings system (Dionex S.A., Voisins-le-Bretonneux, France) coupled to the nano-electrospray II ionisation interface of a QSTAR Pulsar I (Applied Biosystems) using a PICOTip (10 μm internal diameter, New Objectives). Bound peptides were eluted with a gradient of 5–50% of solvent B [20/80 water/acetonitrile in 0.085% (w/v) formic acid]. Information-dependent acquisition was used to acquire MS/MS data, with experiments designed so that the two most abundant peptides were subject to collision-induced dissociation, using nitrogen as the collision gas, every 5 seconds. Data were searched using MASCOT (Matrix Science) software on the NCBI nr *Drosophila melanogaster* database. All data were manually verified in order to minimise errors in protein identification and characterisation.

Electroporation of purified Rac protein

For protein electroporation, GST-Rac1Q61L was purified from *Escherichia coli* BL21* (Invitrogen) and Rac1Q61L cleaved off the GST using thrombin (Sigma). Rac1Q61L was stored at −80℃ in (20 mM Hepes, 100 mM KCl, 5 mM $MgCl_2$, pH 7.7). HeLa cells were trypsinised and resuspended at 25×10^6 cells/ml in DMEM containing 10% FCS and 15 mM Hepes pH 7.5. Cells (200 µl) were mixed with 50 µl purified Rac1Q61L (40 µg). Cells were pulsed at 240 V and 950 µF in a 0.4 cm wide cuvette using a BTX ECM630 electroporator (Harvard Apparatus). Cells were then quickly resuspended in the same medium, washed once, and plated for 2 hours onto glass coverslips or Petri dishes.

For pull-down of active Rac, GST fused to the CRIB domain of PAK was purified from *E. coli* BL21*. Electroporated cells (5×10^6), spread on Petri dishes, were lysed with 500 µl of a solution containing 20 mM Tris-HCl, 150 mM NaCl, 10 mM $MgCl_2$, 1% Triton X-100, pH 7.5. The clarified lysate was then incubated with 10 µl of glutathione beads (4B, GE Healthcare) and 5 µg of GST or GST-CRIB for 2 hours at 4℃. Beads were quickly washed four times in the lysis buffer and resuspended in SDS loading buffer.

Imaging

HeLa and meningioma cells were plated for 2 hours onto glass coverslips coated with 20 µg/ml of collagen type I (BD Biosciences) or 50 µg/ml of fibronectin (Sigma), respectively. Fixed cells were imaged by epifluorescence microscopy on an AxioObserver Z1 microscope (Zeiss) equipped with a 63× NA 1.4 oil immersion objective and an Orca-R^2 camera (Hamamatsu). Where indicated, confocal optical sections were acquired with either of the following custom spinning disc confocal microscopes. The first one is based on a Nikon TE2000-U inverted microscope, a Yokogawa CSU22 spinning disk head, a 100× NA 1.45 oil immersion objective and a CoolSnap HQ2 camera (Photometrics), operated with Metamorph 7.1.4 software (Molecular Devices). The second one is based on a Nikon Eclipse Ti inverted microscope, a Yokogawa CSU-X1 spinning disk head, a 100× NA 1.40 oil immersion objective and an Evolve camera (Photometrics), operated with Metamorph 7.4 software. A maximum intensity z-projection was calculated between five consecutive planes separated by 200 nm. The TIRF microscope was based on a Nikon Eclipse Ti inverted microscope, a TIRF 60× NA 1.49 PlanAPO oil immersion objective, 491 nm and 561 nm lasers and a CoolSnap HQ2 camera (Photometrics), operated with Metamorph 7.6 software. Binning was always set to 1.

For time-lapse microscopy, Swiss 3T3 cells plated onto glass coverslips were placed into chambers for live-cell imaging. Cells were observed with a Nikon Eclipse-Ti microscope equipped with a Plan-Neofluar 40× NA 1.3 DIC objective at 37℃. Images were acquired with an ORCA-ER camera (Hamamatsu) operated with NIS-Elements AR2.3 software (Nikon). To analyse lamellipodial dynamics at the active cell edge, sequences were acquired for 10 minutes at 3 second intervals.

For the migration assay, we used a custom-made microfluidic device composed of 96 holes of 700 µm diameter (Micronit Microfluidics, PV Enschede, The Netherlands), which was applied for 1 hour onto glass coverslips to seed islands of GFP-transfected cells. Then coverslips were either fixed, or incubated for 24 hours before fixation. Images of the GFP signal and DAPI staining were acquired with a 10× objective. The proportion of transfected cells that had migrated outside the original circle was then calculated.

Image analysis and statistics

Analyses of images and movies were performed using ImageJ, Adobe Photoshop and Adobe Premiere software. Gamma settings were not adjusted. For measurements of CHC intensity, images were acquired with the same settings and the intensity was measured using ImageJ after background subtraction. Cell area was measured after manual thresholding of the cortactin staining using ImageJ. Spikes were counted visually. For all quantifications, a minimum of 50 cells of a representative experiment were analysed in each condition. Variations in cell area in independent experiments precluded the averaging of different experiments, but all experiments were repeated between two and six times.

Kymographs were generated along a one-pixel-wide line oriented in the direction of protrusions, using ImageJ. For quantitative analysis, straight lines were drawn on kymographs from the beginning to the end of individual protrusions. Projections along the distance axis and the time axis, gave, respectively, the length and the duration of protrusion. The velocity of protrusion is the ratio between this length and duration. Cycles of protrusion followed by retraction were visually identified. The frequency was calculated by dividing the number of cycles by the duration of acquisition. For each transfection, seven cells were analysed with one to three kymographs per cell. Each kymograph shows several protrusive cycles giving a total ranging from 38 to 47 cycles in the different conditions.

All statistics were performed using SigmaStat software (SPSS). ANOVA was followed by pairwise comparisons using the Student–Newman–Keuls method, with an α factor set to 0.05. When the requirements of normality or equal variance parameters failed to pass, statistics were performed on $\log_{10}$ transformations, which gave normal data sets with equal variance.

Acknowledgments

We thank Philippe Benaroch, Laurence Goutebroze, Christophe Lamaze, Peter Lowe and Theresia Stradal for providing essential reagents. We thank Vic Small for sharing his unpublished assay for cell migration and Thomas Lecuit for suggesting the myristoylated CHC experiment. We thank Cathy Jackson for critical reading of the manuscript. We acknowledge the Developmental Studies Hybridoma Bank developed under the auspices of the NICHD and maintained by the University of Iowa.

Funding

This work was supported by fellowships from the Ministère de l'Education et de la Recherche (to J.J.G. and E.D.); Ligue Nationale contre le Cancer (to L.B.O.); Agence Nationale pour la Recherche [grant number ANR-07-JCJC-0089-01 to A.E.]; University College of London (to B.B.); the Royal Society (to B.B.) and the Ludwig Institute for Cancer Research (to B.B.); the Russian Foundation for Basic Research [grant number 08-04-00452-a to A.Y.A.]. A.G. is supported by Fondation pour la Recherche Médicale; Association pour la Recherche sur le Cancer; and Agence Nationale pour la Recherche [grant numbers ANR-08-BLAN-0012-03, ANR-08-PCVI-0010-03].

Supplementary material available online at
http://jcs.biologists.org/lookup/suppl/doi:10.1242/jcs.081083/-/DC1

References

Abercrombie, M., Heaysman, J. E. and Pegrum, S. M. (1970). The locomotion of fibroblasts in culture. I. Movements of the leading edge. *Exp. Cell Res.* **59**, 393-398.

Anitei, M., Stange, C., Parshina, I., Baust, T., Schenck, A., Raposo, G., Kirchhausen, T. and Hoflack, B. (2010). Protein complexes containing CYFIP/Sra/PIR121 coordinate Arf1 and Rac1 signalling during clathrin-AP-1-coated carrier biogenesis at the TGN. *Nature Cell Biol.* **12**, 330-340.

Billadeau, D. D., Nolz, J. C. and Gomez, T. S. (2007). Regulation of T-cell activation by the cytoskeleton. *Nat. Rev. Immunol.* **7**, 131-143.

Bouslama-Oueghlani, L., Echard, A., Louvard, D. and Gautreau, A. (2007). RNAi depleted Drosophila cell extracts to dissect signaling pathways leading to actin polymerization. *J. Biochem. Biophys. Methods* **70**, 663-669.

Cai, L., Makhov, A. M., Schafer, D. A. and Bear, J. E. (2008). Coronin 1B antagonizes cortactin and remodels Arp2/3-containing actin branches in lamellipodia. *Cell* **134**, 828-842.

Calabia-Linares, C., Robles-Valero, J., de la Fuente, H., Perez-Martinez, M., Martin-Cofreces, N., Alfonso-Perez, M., Gutierrez-Vazquez, C., Mittelbrunn, M., Ibiza, S., Urbano-Olmos, F. R. et al. (2011). Endosomal clathrin drives actin accumulation at the immunological synapse. *J. Cell Sci.* **124**, 820-830.

Dai, J., Ting-Beall, H. P. and Sheetz, M. P. (1997). The secretion-coupled endocytosis correlates with membrane tension changes in RBL 2H3 cells. *J. Gen. Physiol.* **110**, 1-10.

Derivery, E. and Gautreau, A. (2010). Generation of branched actin networks: assembly and regulation of the N-WASP and WAVE molecular machines. *BioEssays* **32**, 119-131.

Derivery, E., Fink, J., Martin, D., Houdusse, A., Piel, M., Stradal, T. E., Louvard, D. and Gautreau, A. (2008). Free Brick1 is a trimeric precursor in the assembly of a functional wave complex. *PLoS ONE* **3**, e2462.

Derivery, E., Lombard, B., Loew, D. and Gautreau, A. (2009). The Wave complex is intrinsically inactive. *Cell Motil. Cytoskeleton* **66**, 777-790.

Dugast, M., Toussaint, H., Dousset, C. and Benaroch, P. (2005). AP2 clathrin adaptor complex, but not AP1, controls the access of the major histocompatibility complex (MHC) class II to endosomes. *J. Biol. Chem.* **280**, 19656-19664.

Echard, A., Hickson, G. R., Foley, E. and O'Farrell, P. H. (2004). Terminal cytokinesis events uncovered after an RNAi screen. *Curr. Biol.* **14**, 1685-1693.

Enari, M., Ohmori, K., Kitabayashi, I. and Taya, Y. (2006). Requirement of clathrin heavy chain for p53-mediated transcription. *Genes Dev.* **20**, 1087-1099.

Gautreau, A., Ho, H.-y. H., Li, J., Steen, H., Gygi, S. P. and Kirschner, M. W. (2004). Purification and architecture of the ubiquitous Wave Complex. *Proc. Natl. Acad. Sci. USA* **101**, 4279-4283.

Insall, R. H. and Machesky, L. M. (2009). Actin dynamics at the leading edge: from simple machinery to complex networks. *Dev. Cell* **17**, 310-322.

Ismail, A. M., Padrick, S. B., Chen, B., Umetani, J. and Rosen, M. K. (2009). The WAVE regulatory complex is inhibited. *Nat. Struct. Mol. Biol.* **16**, 561-563.

Kiger, A. A., Baum, B., Jones, S., Jones, M. R., Coulson, A., Echeverri, C. and Perrimon, N. (2003). A functional genomic analysis of cell morphology using RNA interference. *J. Biol.* **2**, 27.

Kobayashi, K., Kuroda, S., Fukata, M., Nakamura, T., Nagase, T., Nomura, N., Matsuura, Y., Yoshida-Kubomura, N., Iwamatsu, A. and Kaibuchi, K. (1998).

p140Sra-1 (specifically Rac1-associated protein) is a novel specific target for Rac1 small GTPase. *J. Biol. Chem.* **273**, 291-295.

Kunda, P., Craig, G., Dominguez, V. and Baum, B. (2003). Abi, Sra1, and Kette control the stability and localization of Scar/Wave to regulate the formation of actin-based protrusions. *Curr. Biol.* **13**, 1867-1875.

Lebensohn, A. M. and Kirschner, M. W. (2009). Activation of the WAVE complex by coincident signals controls actin assembly. *Mol. Cell* **36**, 512-524.

Machesky, L. M. and Insall, R. H. (1998). Scar1 and the related Wiskott-Aldrich syndrome protein, WASP, regulate the actin cytoskeleton through the Arp2/3 complex. *Curr. Biol.* **8**, 1347-1356.

Machesky, L. M., Mullins, R. D., Higgs, H. N., Kaiser, D. A., Blanchoin, L., May, R. C., Hall, M. E. and Pollard, T. D. (1999). Scar, a WASp-related protein, activates nucleation of actin filaments by the Arp2/3 complex. *Proc. Natl. Acad. Sci. USA* **96**, 3739-3744.

Miki, H., Suetsugu, S. and Takenawa, T. (1998). WAVE, a novel WASP-family protein involved in actin reorganization induced by Rac. *EMBO J.* **17**, 6932-6941.

Miki, H., Yamaguchi, H., Suetsugu, S. and Takenawa, T. (2000). IRSp53 is an essential intermediate between Rac and WAVE in the regulation of membrane ruffling. *Nature* **408**, 732-735.

Oikawa, T., Yamaguchi, H., Itoh, T., Kato, M., Ijuin, T., Yamazaki, D., Suetsugu, S. and Takenawa, T. (2004). PtdIns(3,4,5)P3 binding is necessary for WAVE2-induced formation of lamellipodia. *Nat. Cell Biol.* **6**, 420-426.

Palamidessi, A., Frittoli, E., Garre, M., Faretta, M., Mione, M., Testa, I., Diaspro, A., Lanzetti, L., Scita, G. and Di Fiore, P. P. (2008). Endocytic trafficking of Rac is required for the spatial restriction of signaling in cell migration. *Cell* **134**, 135-147.

Pollard, T. D. (2007). Regulation of actin filament assembly by Arp2/3 complex and formins. *Annu. Rev. Biophys. Biomol. Struct.* **36**, 451-477.

Raucher, D. and Sheetz, M. P. (1999). Membrane expansion increases endocytosis rate during mitosis. *J. Cell Biol.* **144**, 497-506.

Raucher, D. and Sheetz, M. P. (2000). Cell spreading and lamellipodial extension rate is regulated by membrane tension. *J. Cell Biol.* **148**, 127-136.

Rempel, S. A., Schwechheimer, K., Davis, R. L., Cavenee, W. K. and Rosenblum, M. L. (1993). Loss of heterozygosity for loci on chromosome 10 is associated with morphologically malignant meningioma progression. *Cancer Res.* **53**, 2386-2392.

Robinson, M. S. (2004). Adaptable adaptors for coated vesicles. *Trends Cell Biol.* **14**, 167-174.

Rogers, S. L., Wiedemann, U., Stuurman, N. and Vale, R. D. (2003). Molecular requirements for actin-based lamella formation in Drosophila S2 cells. *J. Cell Biol.* **162**, 1079-1088.

Rohn, J. L., Sims, D., Liu, T., Fedorova, M., Schock, F., Dopie, J., Vartiainen, M. K., Kiger, A. A., Perrimon, N. and Baum, B. (2011). Comparative RNAi screening identifies a conserved core metazoan actinome by phenotype. *J Cell Biol.* **194**, 789-804.

Royle, S. J., Bright, N. A. and Lagnado, L. (2005). Clathrin is required for the function of the mitotic spindle. *Nature* **434**, 1152-1157.

Saint-Pol, A., Yelamos, B., Amessou, M., Mills, I. G., Dugast, M., Tenza, D., Schu, P., Antony, C., McMahon, H. T., Lamaze, C. et al. (2004). Clathrin adaptor epsinR is required for retrograde sorting on early endosomal membranes. *Dev. Cell* **6**, 525-538.

Scita, G. and Di Fiore, P. P. (2010). The endocytic matrix. *Nature* **463**, 464-473.

Sossey-Alaoui, K., Li, X., Ranalli, T. A. and Cowell, J. K. (2005). WAVE3-mediated cell migration and lamellipodia formation are regulated downstream of phosphatidylinositol 3-kinase. *J. Biol. Chem.* **280**, 21748-21755.

Steffen, A., Rottner, K., Ehinger, J., Innocenti, M., Scita, G., Wehland, J. and Stradal, T. E. (2004). Sra-1 and Nap1 link Rac to actin assembly driving lamellipodia formation. *EMBO J.* **23**, 749-759.

Suetsugu, S., Kurisu, S., Oikawa, T., Yamazaki, D., Oda, A. and Takenawa, T. (2006). Optimization of WAVE2 complex-induced actin polymerization by membrane-bound IRSp53, PIP(3), and Rac. *J. Cell Biol.* **173**, 571-585.

Takenawa, T. and Suetsugu, S. (2007). The WASP-WAVE protein network: connecting the membrane to the cytoskeleton. *Nat. Rev. Mol. Cell Biol.* **8**, 37-48.

Weiner, O. D., Neilsen, P. O., Prestwich, G. D., Kirschner, M. W., Cantley, L. C. and Bourne, H. R. (2002). A PtdInsP(3)- and Rho GTPase-mediated positive feedback loop regulates neutrophil polarity. *Nat. Cell Biol.* **4**, 509-513.

Weiner, O. D., Rentel, M. C., Ott, A., Brown, G. E., Jedrychowski, M., Yaffe, M. B., Gygi, S. P., Cantley, L. C., Bourne, H. R. and Kirschner, M. W. (2006). Hem-1 complexes are essential for Rac activation, actin polymerization, and myosin regulation during neutrophil chemotaxis. *PLoS Biol* **4**, e38.

Yamazaki, D., Suetsugu, S., Miki, H., Kataoka, Y., Nishikawa, S., Fujiwara, T., Yoshida, N. and Takenawa, T. (2003). WAVE2 is required for directed cell migration and cardiovascular development. *Nature* **424**, 452-456.

Journal of Cell Science